Heterozygous Loss of *Yap1* in Mice Causes Progressive Cataracts

Qingxian Lu, Yingnan Zhang, Ramesh Babu Kasetti, Subhash Gaddipati, Naresh Kumar CVM, Douglas Borchman, and Qiutang Li

Department of Ophthalmology and Visual Sciences, University of Louisville School of Medicine, Louisville, Kentucky, United States

Correspondence: Qiutang Li, Department of Ophthalmology and Visual Sciences, University of Louisville, 301 East Muhammad Ali Boulevard, Louisville, KY 40202, USA;
q.li@louisville.edu.

Received: February 20, 2020
Accepted: October 1, 2020
Published: October 21, 2020

Citation: Lu Q, Zhang Y, Kasetti RB, et al. Heterozygous loss of *Yap1* in mice causes progressive cataracts. *Invest Ophthalmol Vis Sci.* 2020;61(12):21.
https://doi.org/10.1167/iovs.61.12.21

Purpose. Yap1 encodes an evolutionarily conserved transcriptional coactivator and functions as a down-stream effector of the Hippo signaling pathway that controls tissue size and cell growth. Yap1 contributes to lens epithelial development. However, the effect of *Yap1* haplodeficiency on the lens epithelium and its role in the development of cataracts has not been reported. The aim of the current study is to investigate Yap1 function and its regulatory mechanisms in lens epithelial cells (LECs).

Methods. Lens phenotypes were investigated in *Yap1* heterozygous mutant mice by visual observation and histological and biochemical methods. Primary LEC cultures were used to study regulatory molecular mechanism.

Results. The heterozygous inactivation of *Yap1* in mice caused cataracts during adulthood with defective LEC phenotypes. Despite a normal early development of the eye including the lens, the majority of *Yap1* heterozygotes developed cataracts in the first six months of age. Cataract was preceded by multiple morphological defects in the lens epithelium, including decreased cell density and abnormal cell junctions. The low LEC density was coincident with reduced LEC proliferation. In addition, expression of the *Yap1* target gene *Crim1* was reduced in the $Yap1^{+/-}$ LEC, and overexpression of Crim1 restored $Yap1^{+/-}$ LEC cell proliferation in vitro.

Conclusions. Homozygosity of the *Yap1* gene was critical for adequate *Crim1* expression needed to maintain the constant proliferation of LEC and to maintain a normal-sized lens. *Yap1* haplodeficiency leads to cataracts.

Keywords: lens epithelium, cataracts, Yap1, cell proliferation, Crim1

Elucidating the mechanisms related to the maintenance of lens size and shape is a fundamental biological aim. The ocular lens is an avascular transparent tissue derived from lens epithelial cells (LEC).[1,2] During development, the ectoderm of the embryonic sensory placodes first form the lens pit, and then the lens vesicle, from which the cells at the anterior region differentiate into LEC. LEC near the lens equator divide and differentiate into secondary fiber cells.[3,4] Meanwhile, cells from the posterior region of the lens elongate to form primary lens fibers.[5] In contrast to most tissues, the lens grows continuously throughout life with very low turnover of proteins or lipids in mature lens fiber cells.[6–8] Thus the lens becomes larger with age. The slow postnatal growth of the lens is achieved by cell division that occurs on a very limited scale in a loosely defined band of epithelial cells in the germinative zone, just above equator. These daughter cells move to the transition zone below the equator where they differentiate into fiber cells that incorporate into the fiber cell mass.[3,6,9] The correct proliferation of LEC is essential for maintaining normal cellular homeostasis and lens size. Molecular mechanisms underlying lens development including induction, morphogenesis, differentiation, and growth have been investigated extensively.[4,10–13] The Hippo pathway is an evolutionally conserved key regulator for tissue size control.[14] Yap and Taz are the major downstream effectors of the Hippo pathway. The loss of Hippo pathway activity or increased activation of Yap results in increased cell proliferation and tissue overgrown in the epithelia of the Drosophila eye discs and in the liver, intestine, bronchus, and skin of mice.[15–21] *Yap1* null mice die at embryonic day 8.5 with defects in yolk sac vasculogenesis, chorioallantoic attachment, and embryonic axis elongation.[22] Deletion of *Yap1* in the intestine or bronchus of *Yap1*-conditional knockout mice revealed a mild phenotype related to proliferative repair and the reduction of stem cells.[21,23] Dysregulation of the Hippo-Yap pathway has been linked to tumor progression and cancer development, and eye disorders such as ocular colobomas, Sveinsson chorioretinal atrophy (SCRA; OMIM no. 108985), and retinal degeneration.[24–29]

A defective lens phenotype in the Nestin-Cre-driven Merlin/NF2 conditional knockout mice was largely suppressed by heterozygous deletion of Yap, which suggests a potential functional role of Hippo/Yap- signaling in lens development.[30] Yap activity is essential for maintenance of LEC progenitor activity by preserving self-renewal, and

inhibiting apoptosis and precocious differentiation.[31,32] In addition, Yap plays a crucial role in maintaining LEC and fiber morphology via stabilizing apical polarity complex and junctional proteins.[32] Inhibition of YAP with Verteporfin suppressed FGF-induced lens cell proliferation and ablated cell elongation during lens fiber differentiation.[33] Furthermore, YAP1 regulates LEC proliferation and fibrogenic response induced by mechanotransduction of stress.[34–36] However, the molecular mechanism of Yap1 in maintaining homeostasis in the mature lens remains largely unexplored.

YAP1 controls cell proliferation through its nuclear transcriptional coactivation activity that regulates TEAD transcriptional function. A number of genes have been identified as YAP1 targets, including Crim1.[37–41] CRIM1 is a type I transmembrane protein and has been studied in relation to cancer cell migration and invasion.[42] It is important for the maintenance of LEC polarity, proliferation, and adhesion interactions during lens development that most likely involves integrin signaling.[43] Lower levels of CRIM1 leads to the abnormal transition of LEC into fibers.[44] CRIM1 haploinsufficiency was implicated in the human ocular syndrome MACOM (OMIM no. 602499).[45] Here, we present a phenotypic analysis of *Yap1* heterozygous mice to determine the role of Yap1 in LEC proliferation and homeostasis with mechanistic involvement of Crim1.

Materials and Methods

Ethics Statement

All animal experiments were approved by Institutional Animal Care and Use Committee at the University of Louisville and were conducted in accordance with the guidelines of the Association for Research in Vision and Ophthalmology on the use of animals in research.

Mice and Genotyping

C57BL/6J mice were purchased from The Jackson Laboratory (Bar Harbor, ME, USA) and used to set up a breeding colony. The *Yap1*$^{+/-}$ mice on the C57BL/6 background were purchased from the International Knockout Mouse Consortium (UC Davis, Davis, CA, USA). Mice were housed under pathogen-free conditions and handled in accordance with guidelines approved by the Institutional Animal Care and Use Committee of the University of Louisville. Genotypes were determined by performing PCR amplification based on the information provided by vendors.

Histology and Immunostaining

Mice were euthanized by CO_2 asphyxiation followed by cervical dislocation. Enucleated eyes were fixed in 4% paraformaldehyde in phosphate buffered saline, pH 7.4, overnight before embedding in either optimal cutting temperature compound or paraffin. The paraffin-embedded tissues were sectioned at a thickness of 7 µm and prepared for hematoxylin and eosin staining. For immunohistochemistry, the tissue sections or cultured cell preparations were subjected to an antigen-retrieval procedure by heating the slides at 95°C for 30 minutes in 10 mM Tris-EDTA buffer (pH 9.0). The primary antibodies used in this study were mouse anti-YAP1 (1:100, cat. no. 56701; Abcam, Cambridge, MA, USA), mouse anti YAP1 (1:100, cat. no. sc-101199; Santa Cruz Biotechnology, Santa Cruz, CA, USA), mouse anti-β-catenin (1:100, cat. no. BD 610154; BD Bioscience, Franklin Lakes, NJ, USA), rabbit anti-β-catenin (D10A8) (1; 100, cat. no. 8480S; Cell Signaling Technology, Danvers, MA, USA), rabbit anti-ZO-1 (1:200, cat. no. 61-7300; Thermo Fisher Scientific, Waltham, MA, USA), rabbit anti-βB1-crystallin (1:200, cat. no. NBP2-68576; Novus Biologicals, Centennial, CO, USA), rabbit anti-Crim1 (1:100, cat. no. AB5699, Millipore Sigma, Burlington, MA, USA), rat anti-BrdU (1:800, MAS 250c, Harlan-Sera Lab, Belton Loughborough, Leicestershire, UK). The secondary antibodies, conjugated with either carbocyanine 3 or fluorescein isothiocyanate, were purchased from Jackson ImmunoResearch Laboratories, Inc. (West Grove, PA, USA). The fluorescent images were examined and photographed using a Zeiss Axio Imager M2 system equipped with ApoTome, AxioCam and AxioVision (Zeiss, Peabody, MA, USA) or FV3000 confocal laser scanning microscope (Olympus, Center Valley, PA, USA).

TUNEL Assay

The eye tissue sections from four-week-old wild-type and *Yap1*$^{+/-}$ mice were used for detecting apoptotic cells by in situ terminal transferase dUTP nick end labeling (TUNEL) using an APO-BRDU-IHC (TUNEL) Apoptosis Kit (cat. no. NBP2-31164; Novus Biologicals) following the manufacturer's instructions. BrdU incorporation was detected by rat anti- BrdU antibody and carbocyanine 3 conjugated secondary antibody. The fluorescent-labeled apoptotic cells were observed and photographed using a FV3000 confocal laser-scanning microscope (Olympus, Center Valley, PA, USA). LEC and fibers of six independent specimens from both wild type (WT) and *Yap1* ckO specimens were examined using the TUNEL assay.

Lens Dissection and Imaging

Lenses were dissected under a dissecting microscope. The sclera and retina were peeled off from the optic nerve using a pair of forceps. The iris and ciliary body were carefully removed from the lens by cutting the zonules with micro scissors. Immediately after dissection, the lenses were submerged in medium and photographed under a dissection microscope (Zeiss Discovery 8 Stereomicroscope) equipped with an advance digital camera. A ring light was used for intense and focused shadow-free illumination for photography. The dishes containing lenses were placed on grid paper and then photographed.

BrdU Labeling of Proliferative Cells in Vivo and BrdU Detection

Mice were injected with BrdU intraperitoneally (150 mg/kg body weight), and sacrificed two hours later. Eyes were enucleated and fixed in 4% paraformaldehyde at 4°C for 24 hours. Whole lenses were dissected and the antigen retrieval procedures followed as described above. Anti-BrdU primary antibody was used to detect the BrdU incorporated cells, and visualized by fluorescent-dye conjugated secondary antibodies. Nuclei were stained by 4′,6-diamido-2-phenylindole (DAPI). Lens capsules were peeled off and placed on glass slides with the epithelium facing up, and mounted in Vectashield fluorescence mounting medium (Vector Labs, Burlingame, CA, USA). The fluorescent images were examined and photographed using a Zeiss Axio Imager

Investigative Ophthalmology & Visual Science

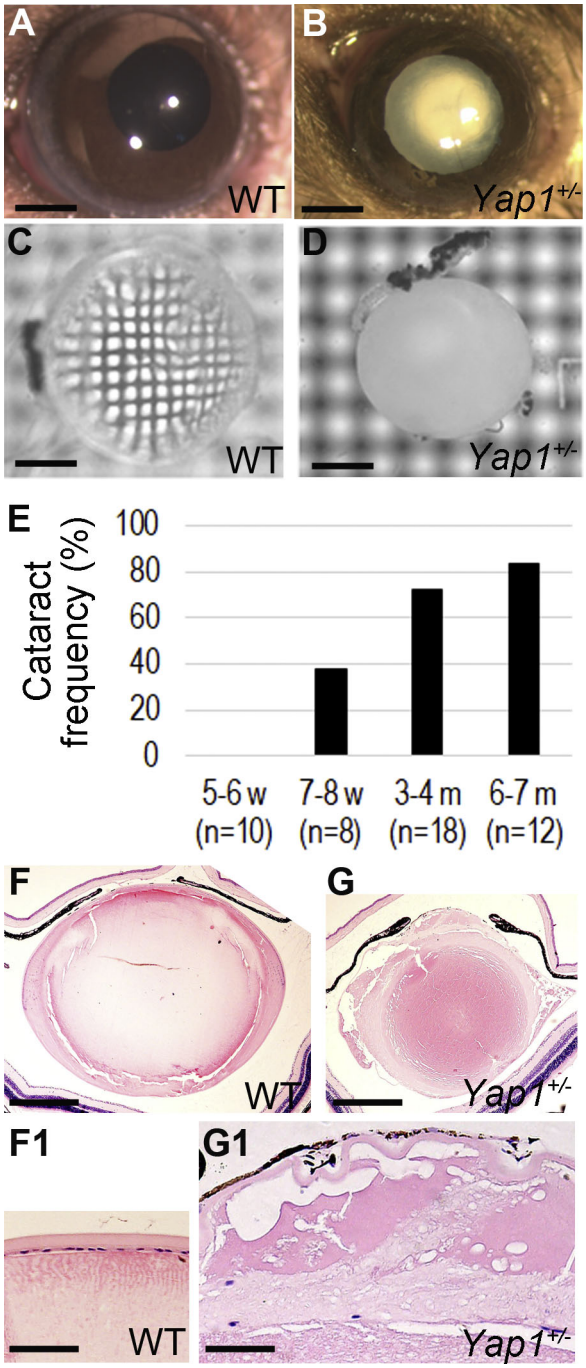

Figure 1. Development of cataracts in the *Yap1*$^{+/-}$ mice. (**A**, **B**) Images of WT eye (**A**) and the cataract eye of *Yap1*$^{+/-}$ mouse (**B**) at two months of age. (**C**, **D**) Transparency of freshly collected lenses. The lenses were placed on the grid papers and photographed by transillumination with white light. Transparency is indicated by the clarity of grid. (**E**) Percentage of the animals at each age group that developed cataracts. Note that each age group is a separate cohort of mice. (**F**, **G**) Histological hematoxylin and eosin staining of paraffin-embedded eye sections from WT and *Yap1*$^{+/-}$ cataract mice at three months old. The cortical rupture in *Yap1*$^{+/-}$ lens was noticeable in **G**. (**F1**, **G1**) High-magnification views of **F** and **G**, respectively. *Scale bar*: 500 µm (**A–D**, **F**, and **G**), 50 µm (**F1** and **G1**).

M2 system with ApoTome, AxioCam, and AxioVision (Zeiss, Peabody, MA, USA). The number and percentage of BrdU-positive cells at the germinative zone were counted in lens epithelial capsule explants from three mice in each experimental group, and at least three images were used for counting the BrdU-positive cells for each mouse. All data were summarized as the mean ± SD. A two-tailed Student *t*-test was performed to determine the significance of the differences between means. The differences were considered statistically significant if the *P* values were less than 0.05.

LEC Culture and BrdU Labeling and Detection

For preparation of primary LEC cultures, lenses were isolated from euthanized five-week-old WT and *Yap1*$^{+/-}$ mice. LEC were isolated following the methods previously published.[46,47] Briefly, lenses were placed in a cell culture dish containing medium 199 supplied with 0.1% bovine serum albumen, 100 U/mL penicillin, 100 µg/mL streptomycin, and 2.5 µg/mL amphotericin B. To obtain capsule-epithelial whole-mounts, lenses were placed posterior-side up, and the posterior capsule was torn by sharp forceps. The capsule with adherent epithelial cells was then removed from the fiber mass. The capsules were collected into a 1.5 mL test tube and centrifuged for five minutes at 2000 rpm. The suspension medium was removed carefully, and 300 µL of 0.05% trypsin was added. After shaking for 10 minutes, the cells were washed once in phosphate-buffered saline solution and collected by centrifugation. The cell pellets were resuspended in suspension medium (including FGF2, 100 ng/mL), transferred into 24-well plates (for Western blotting) or an eight-chamber slide (for immunostaining), and incubated at 37°C and 5% CO_2. To facilitate attachment to the surface of the plates, the cells were washed with 100% fetal bovine serum before being placed into the culture dishes. After two days in culture, the cells were transduced overnight with lentivirus carrying Crim1 cDNA or control lentivector (without cDNA insertion). The medium was replaced with fresh medium the next day. Two days after lentiviral transduction, the LEC in the 24-well plates were collected into the protein lysis buffer and analyzed by Western blotting. LEC were placed on eight-chamber-slides and labeled with 10 µM BrdU for 2 hours before being fixed with 4% paraformaldehyde for 15 minutes and processed for anti-BrdU immunostaining.

Lentiviral Production

Crim1 cDNA in lenti-vector was obtained from GeneCopoeia (cat. EX-Mm06868-Lv121; Rockville, MD, USA). The detailed production procedure using lentiviral expression vectors has been published previously.[48] Lentivirus was collected in LEC culture medium and directly used to transduce the primary LEC for overnight.

RNA Isolation and Quantitative (q) PCR

Lens capsule-epithelial whole-mount sheets were peeled off the lens with forceps, and immediately immersed in TrIzol reagent (Thermo Fisher Scientific) after removing attached lens fibers. Total RNA was extracted from the pooled LEC samples prepared from 5–8 WT or *Yap1*$^{+/-}$ mice using RNeasy mini column (QIAGEN, Germantown, MD, USA). For each experiment, quantitative polymerase chain reaction

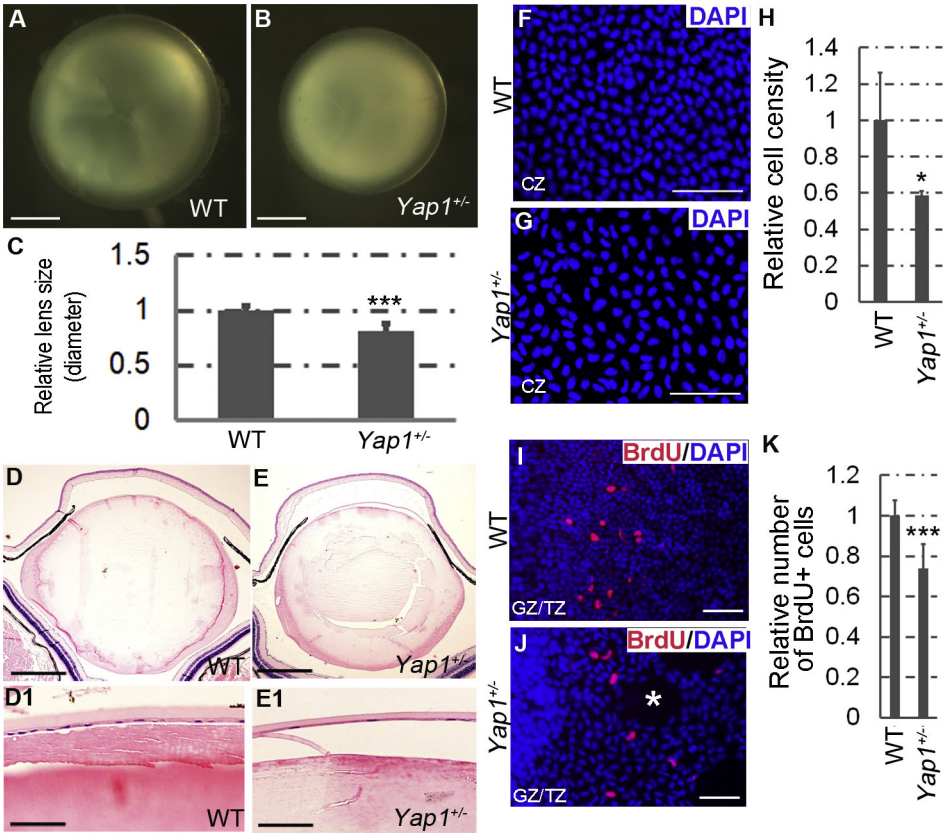

Figure 2. Reduction of lens size, LEC density, and LEC proliferation in *Yap1*$^{+/-}$ mice. Experiments were performed on one-month-old WT and *Yap1*$^{+/-}$ sibling mice. (**A**, **B**) Images of the freshly isolated lenses from WT and *Yap1*$^{+/-}$ mice show difference in lens size. (**C**) Quantification of relative lens size based on the diameter of lens (n = 8 mice for each group). (**D**, **E**) Hematoxylin and eosin staining of eye sections from WT and *Yap1*$^{+/-}$ mice. (**D1–E1**) High-magnification views of D and E, respectively. (**F**, **G**) Fluorescent images taken from the central zone (CZ) of flat-mounted lens epithelium stained with DAPI to identify cell nuclei. (**H**) Relative cell density calculated by the number of cell nuclei per equal unit of area using Image J software (n = 5 mice for each group). (**I**, **J**) Fluorescent images taken from the germinative zone (GZ) and transitional zone (TZ) of lens immunostained with anti-BrdU antibody (*red*) and nuclear counterstained with DAPI (*blue*). (**K**) Relative number of BrdU^{+} cells in WT and *Yap1*$^{+/-}$ mice. The quantitative analysis of representative images was conducted using Image J software. The numbers of BrdU^{+} cell were normalized by the distance along equatorial plane (n = 6 mice for each group). * $P < 0.05$. *** $P < 0.005$. *Scale bar:* 500 µm (**A**, **B**, **D**, and **E**), 50 µm (**D1**, **E1**, **F**, **G**, **I**, and **J**). * indicates large breakdown of lens epithelium. All values are expressed as the mean ± SD.

(qPCR) was done in triplicate, and at least three independent samples were used. The $2^{-\Delta\Delta CT}$ method was used to analyze relative gene expression, which was normalized to the *Actb* gene.[49] Primers for mouse *Yap1* (ID: 15928514a1) and mouse *Crim1* (ID: 293651551c3) were designed based on the Primer Bank online database (Harvard Medical School, Boston, MA, USA; http://pga.mgh.harvard.edu/primerbank). *Actb* primers were previously reported.[50]

Western Blot Analysis

Lenses were immediately dissected under a dissecting microscope from the enucleated eyes of euthanized four- to five-week-old mice. After removing surrounding tissue, lens capsules were peeled off by forceps and transferred into a cold radio immunoprecipitation assay buffer plus protease inhibitor cocktail tablets (Roche), and equal amounts of cell lysates were separated by 8% to 10% sodium dodecyl sulfate-polyacrylamide gel electrophoresis and transferred to nitrocellulose membranes. After incubation in blocking buffer consisting of 10 mM Tris, pH 8, 150 mM NaCl, 0.1% Tween 20 (TBST), and 5% nonfat milk for 30 minutes at room temperature, the blot was incubated with the primary antibodies in the blocking buffer at room temperature for 2 hours. The antibodies used in Western analysis included mouse anti-YAP1 antibody (1:100, cat. no. sc-101199; Santa Cruz Biotechnology), rabbit anti-CRIM1 (1:100, cat. no. AB5699; Millipore Sigma), mouse anti-α-TUBULIN antibody (1:500 dilution; Sigma, T9026), rabbit anti-FAK (1:250, cat. no. 13009; Cell Signaling Technology), rabbit anti-phospho-FAK (Tyr397) (1:250, cat. no. 8556; Cell Signaling Technology), rabbit anti-ERK1/2 (1:250, cat. # 137F5; Cell Signaling Technology), and goat anti-phospho-ERK1/2 (Thr 202/Tyr 204) (1:100, cat. no. sc-101199, Santa Cruz Biotechnology). After three washes in TBST, the membranes were incubated for 30 minutes at room temperature with the appropriate secondary antibody conjugated to horseradish peroxidase (Amersham Biosciences. Piscataway, NJ, USA) in blocking buffer. Following three washes with TBST, the blots were visualized with an enhanced chemiluminescence system (Amersham Biosciences).

Statistical Analysis

Data are reported as the mean ± SD, n = 3–14 mice. Normality of data was confirmed by the Shapiro-Wilk test. Statistical

Investigative Ophthalmology & Visual Science

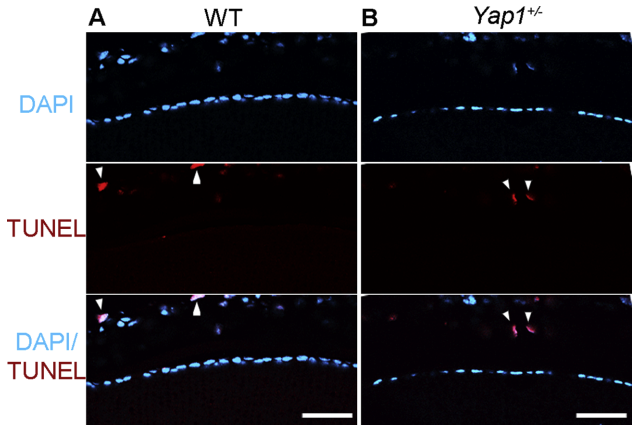

Figure 3. No apoptosis induction in *Yap1*$^{+/-}$ lens epithelium. Experiments were performed on one-month-old WT and *Yap1*$^{+/-}$ sibling mice. Six mice from each group and six sections from each eye were examined. (**A, B**) Representative images of TUNEL assay staining on the lens sections of WT (**A**) and *Yap1*$^{+/-}$ (**B**) mice. *Scale bar:* 50 µm, *arrow heads* indicate the apoptotic cells detected by TUNEL in iris tissue.

comparisons between experimental groups were conducted using the Student *t*-test. $P \leq 0.05$ was considered as statistically significant.

Results

Loss of One Allele of *Yap1* in Mice Leads to Cataracts Soon After Birth

Yap1$^{+/-}$ mice were identified by PCR genotyping, and born in an expected Mendelian ratio. The *Yap1*$^{+/-}$ mice were viable, healthy, and fertile, but appeared smaller than their WT littermates at 1-month-old. Within the first few months after birth, the Yap1$^{+/-}$ mice developed obvious gross lenticular opacities in one or both eyes, whereas no WT littermate controls developed cataracts (Figs. 1A, 1B). The affected lenses became opaque with a cloudy appearance obscuring the underlying grid pattern completely (Figs. 1C, 1D). This phenotype was highly penetrant, appearing in 80% of the animals examined by six months of age (Fig. 1E). Histopathologic examination of the lenses from eight-week-old *Yap1*$^{+/-}$ mice with cataracts (Figs. 1G, 1G1) showed that the lens morphology was severely disrupted, as characterized by capsular and epithelial rupture, numerous large cortical vacuoles, and fragmentation and disruption of lens fibers, but those changes were not seen in the WT controls (Figs. 1F, 1F1).

YAP1 Regulates Lens Size and LEC Density by Controlling LEC Proliferation

To examine the cellular changes that potentially caused cataracts, we analyzed the morphology of the clear lenses in the *Yap1*$^{+/-}$ mice at one month of age. Dark-field microscopy revealed that the average size of *Yap1*$^{+/-}$ lenses was about 81.6% the diameter of the WT lenses (Figs. 2A–C). Lens opacity was not apparent at this time point. Histochemical studies showed that the lens structure was normal, but the density of LEC was significantly lower in the mutant animals compared

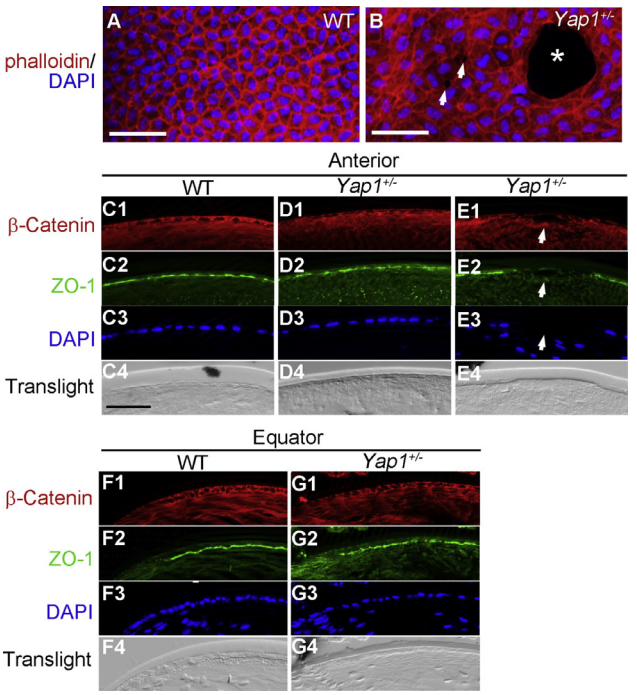

Figure 4. Disruption of cell-cell junctions in *Yap1*$^{+/-}$ lens epithelium. (**A**, **B**) Representative images of flat-mounted lens epithelium stained with phalloidin and DAPI. (**C1–C4**, **D1–D4**, **E1–E4**) The representative images at anterior of WT (**C1–C4**) and *Yap1*$^{+/-}$ (**D1–D4**, **E1–E4**) lenses immunostained with antibodies against β-catenin and ZO-1, with DAPI counterstaining to show cell nuclei. (**F1–F4**, **G1–G4**) The representative images at equator of WT (**F1-F4**) and *Yap1*$^{+/-}$ (**G1–G4**) lenses immunostained with antibodies against β-catenin and ZO-1, and DAPI to counterstained nuclei. Six mice per group were used for each experiment.

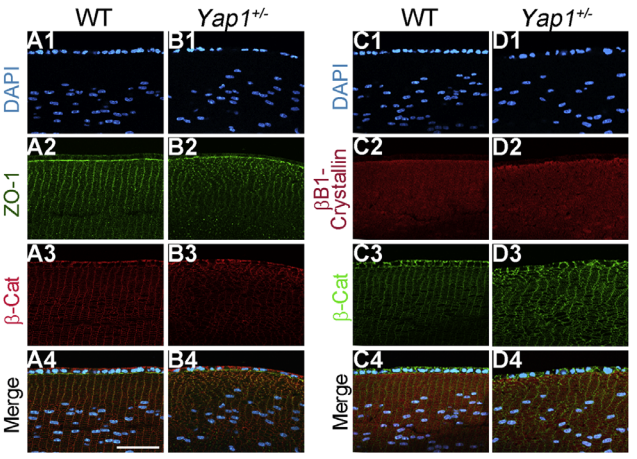

Figure 5. Disrupted lens fiber morphology and normal βB1-crystallin expression in *Yap1*$^{+/-}$ lens. Experiments were performed on one-month-old WT and *Yap1*$^{+/-}$ sibling mice. Six mice from each group and at least six transverse sections around the germinative zone from each eye were examined. (**A**, **B**) Representative images of transverse sections of lenses immunostained with antibodies against β-catenin and ZO-1 with nuclear counter staining by DAPI. (**C**, **D**) Representative images of transverse sections of lenses immunostained with antibodies against βB1-crystallin, β-catenin, with DAPI nuclear counter-staining to show cell nuclei. All images are in the same magnification. *Scale bar:* 50 µm.

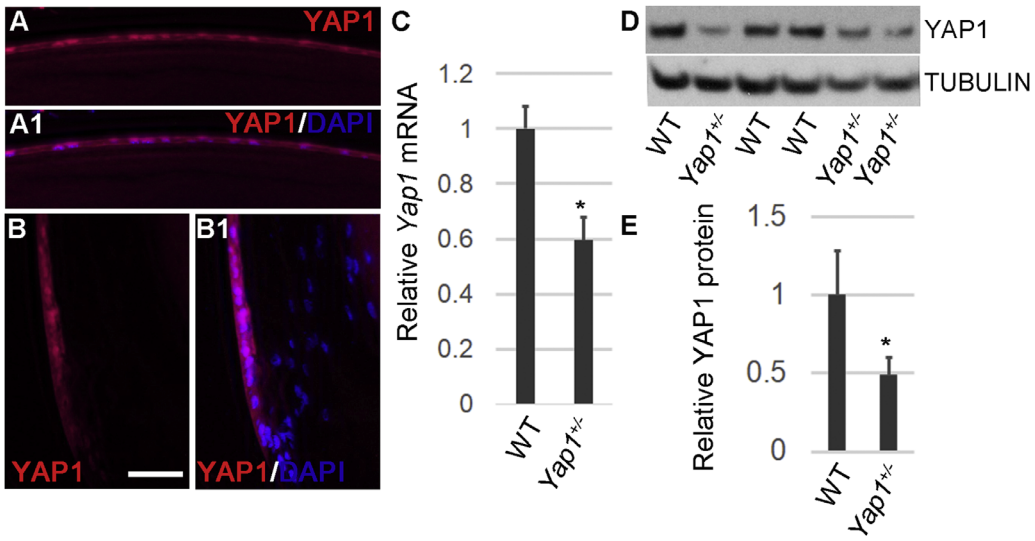

Figure 6. YAP1 expression in WT and *Yap1*$^{+/-}$ lens epithelia. (**A–A1**, **B–B1**) Immunostaining of YAP1 (*red*) and counter-stained with DAPI (*blue*) on anterior (**A–A1**) and equator (**B–B1**) of the WT lenses. *Scale bar:* 50 µm. (**C**) qPCR analysis of *Yap1* mRNA in the lens epithelium of WT and *Yap1*$^{+/-}$ eyes, showing a significant reduced *Yap1* mRNA in the heterozygous mutant lenses. The comparative threshold cycle (CT) methods normalized to *Actb* were used to analyze relative changes in gene expression. The relative expression (arbitrary units) is expressed as a ratio (n = 3 independent samples). Each total RNA sample was isolated from lens epithelial cells pooled from five to eight mice (10–16 lenses), and qPCR analysis for each sample was performed in triplicate. * $P < 0.05$. (**D**) Representative Western blotting shows YAP1 protein expression level in the WT and *Yap1*$^{+/-}$ lens epithelia. Alpha-TUBULIN is used as loading control. (**E**) The quantification of relative YAP1 protein level was normalized to α-TUBULIN protein level after quantification of Western blot images using Image J software (n = 3). Each sample was pooled from five to eight mice, * $P < 0.05$. All values are expressed as the mean ± SD.

with WT animals (Figs. 2D–D1 vs. 2E-E1). To quantify LEC number, we stained the intact lenses in the whole-mounts with DAPI and determined LEC density by counting the DAPI stained nuclei (Figs. 2F–G). The LEC density of the mutant lenses was approximately 32% lower compared with the WT controls (Fig. 2H). Because the adult LEC are produced by proliferation at the germinative zone, slightly above the lens equator, we studied the cell proliferation in the mutants by BrdU incorporation assay and anti-BrdU antibody immunostaining (Figs. 2I–J). The mutant lenses exhibited a 26% reduction of the BrdU labeled proliferating cells in the peripheral region of the explants compared with the WT controls (Fig. 2K). In addition, there were a number of acellular gap areas at the peripheral region of the mutant explants (Fig. 2J, indicated by *), indicating epithelial breakdown.

Given that Yap1 plays an important role in preventing cell apoptosis, we performed TUNEL assays to test whether increased apoptosis contributes to LEC density reduction in the *Yap1*$^{+/-}$ lens. No apoptosis in both WT and *Yap1*$^{+/-}$ lens epithelia was detected (Figs. 3A and 3B), whereas apoptotic cells were readily detectable in adjacent iris tissues (Figs. 3A, 3B), which served as a positive control for the TUNEL assay. This was consistent with previous studies, which showed that TUNEL staining was rarely detectable in the normal healthy lens epithelium.[6,9,51] No apoptosis induction in the *Yap1*$^{+/-}$ LEC, as shown by the TUNEL assay, suggested that the loss one allele of *Yap1* was not sufficient to induce cell apoptosis in LEC in vivo. Taken together, these results demonstrate that decreased LEC proliferation is the primary cause for reduced lens size and LEC density in *Yap1*$^{+/-}$ mice.

YAP1 Regulates LEC Junction and Fiber Morphogenesis

To elucidate the underlying mechanisms that cause disorders in LEC integrity, we evaluated whole-mount lens epithelial sheets that were labeled with rhodamine-phalloidin to reveal the actin cytoskeleton. In contrast to the normal LEC that were shaped regularly with a sharp F-actin network at cell boundaries (Fig. 4A), *Yap1*$^{+/-}$ LEC were disorganized with disrupted cell adhesion (Fig. 4B, indicated with white arrows) and large acellular holes (Fig. 4B, indicated with *). We then measured the expression and localization of the key cell-cell contact molecules in lens sections, including tight junctional protein ZO-1 and the adherens junction associated protein, β-catenin found in the lens membranes. Immunostaining of anti-ZO-1 antibody revealed local disruption of the tight junctions (Figs. 4C–G) at the anterior and equatorial regions of the lens. Similarly, anti-β-catenin immunostaining showed a discontinuity in the mutant LEC (Figs. 4C–G). Consistent with the whole mount observation in Fig. 4B, the disruption and loss of LEC was detected in mutant lens cross sections (Figs. 4E1–E4, indicated with white arrows).

We also examined the cell adhesion marker ZO-1 and β-catenin in the transverse sections around the germinative zone. The fibers were disorganized in the mutant lenses, in contrast to an ordered fiber alignment of hexagonal cross sections in the WT control lenses suggesting an abnormal alignment and irregular packing of fibers in the *Yap1*$^{+/-}$ lens (Figs. 5A and 5B). To further examine the *Yap1*$^{+/-}$ fiber differentiation, we performed βB1-crystallin -labeling staining on the lenses of both *Yap1*$^{+/-}$ and WT control mice. βB1-crystallin was detected only in the fiber cells but not in LEC

in both WT and *Yap1*$^{+/-}$ lenses, suggesting *Yap1*$^{+/-}$ lenses differentiated normally (Figs. 5C and 5D).

YAP1 is Expressed in the Nuclei of Lens Epithelia and Reduced in the *Yap1*$^{+/-}$ LEC

YAP1 is a transcriptional coactivator, and its activity is regulated by nucleocytoplasmic shuttling. To correlate YAP1 expression with lens phenotypes in *Yap1*$^{+/-}$ mice, we performed anti-YAP1 immunostaining on the WT lens sections. Expression of YAP1 was detected in the nuclei of LEC at the anterior (Figs. 6A, 6A1) and equatorial regions (Figs. 6B, 6B1). *Yap*1 mRNA expression was 40% lower in *Yap1*$^{+/-}$ LEC compared with the WT LEC (Fig. 6C). The level of YAP1 protein was 51% lower in *Yap1*$^{+/-}$ LEC compared with that of the WT LEC (Figs. 6D, 6E).

YAP1 Regulates *Crim1* Expression in Lens Epithelium

Given that *Crim1* is characterized as a YAP1 target gene in a number of tumor cell lines [37,52–54] and is a critical regulator for lens development and lens epithelial integrity,[43,45,55] we examined *Crim1* expression in the LEC of one-month-old *Yap1*$^{+/-}$ mice. The level of *Crim1* mRNA in *Yap1*$^{+/-}$ LEC was reduced by 33% compared with WT LEC (Fig. 7A), suggesting that YAP1 regulates *Crim1* transcription in LEC. Furthermore, immunostaining showed that the fluorescence intensity of intracellular CRIM1 staining in the *Yap1*$^{+/-}$ LEC appeared lower compared with WT LEC, indicating a decrease in the amount of CRIM1 protein (Fig. 7B). To further quantify the level of CRIM1 protein in LEC, Western blot analysis was performed on the lens epithelia (Fig. 7C) and showed that the level of CRIM1 protein was 67% lower in *Yap1*$^{+/-}$ LEC compared with that of the WT LEC (Fig. 7D). Given that Crim1 interacts with the β1 integrin signaling pathway and regulates phosphorylation of FAK and ERK signaling molecules in mouse LEC,[43] we then examined whether reduction of Crim1 in *Yap1*$^{+/-}$ LEC affected the phosphorylation profiles of FAK and ERK by Western blot analysis (Fig. 7E). Our result showed that the phosphorylation levels of FAK and ERK1/2 in *Yap1*$^{+/-}$ LEC was significantly lower by an average of 44% and 79%, respectively of WT levels (Figs. 7E, 7F).

Overexpression of *Crim1* can Rescue the Defective Proliferation Phenotype in the *Yap1*$^{+/-}$ LECs

To investigate whether CRIM1 functioned downstream of YAP1 in regulating LEC proliferation, we transduced both primary cultured WT and *Yap1*$^{+/-}$ LECs with Crim1-expressing lentiviruses or control lentiviruses to test whether enforced expression of Crim1 would rescue the proliferating phenotype. The BrdU incorporation assay was adopted to evaluate cell proliferation and BrdU incorporation was reduced in the primary *Yap1*$^{+/-}$ LEC compared with the WT LEC controls (Figs. 8C vs. 8A, 8E). Transduction of Crim1-expressing vector dramatically increased LEC proliferation significantly in both WT and *Yap1*$^{+/-}$ LEC (Figs. 8B vs. 8D, 8E) and notably the proliferation rate of *Yap1*$^{+/-}$ LEC reached a level similar to that of the WT LEC (Fig. 8E). Western blot analysis confirmed the overexpression of CRIM1 in the WT and *Yap1*$^{+/-}$ LEC on Crim1-lentiviral transduction

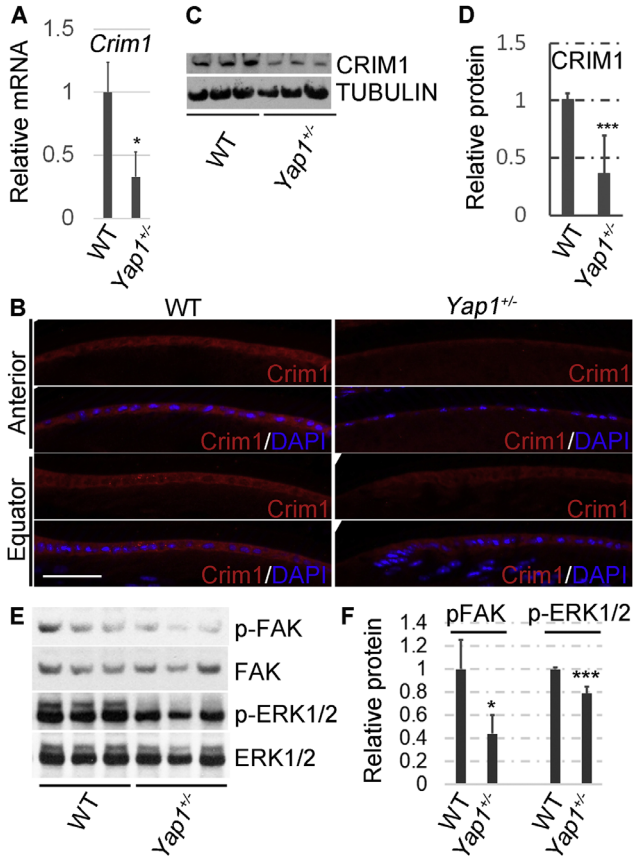

Figure 7. Reduced Crim1 expression in *Yap1*$^{+/-}$ lens epithelium. (**A**) The qPCR quantification of *Crim1* mRNA from the WT and *Yap1*$^{+/-}$ lens epithelia. The comparative threshold cycle methods normalized to Actb were used to analyze relative changes in gene expression. The relative expression (arbitrary units) is presented as a ratio. Data are expressed as mean ± the SD (n = 3 independent samples), each sample was total RNA isolated from lens epithelium pooled from five to eight mice (10–16 lenses), and qPCR analysis for each sample was performed in triplicate. * $P < 0.05$. (**B**) Immunostaining with anti-CRIM1 antibody (*red*) and DAPI (*blue*) on WT and *Yap1*$^{+/-}$ lens epitheliums. *Scale bar:* 50 µm. (**C**) Representative Western blotting on the protein samples from WT and *Yap1*$^{+/-}$ lens epithelia. Alpha-TUBULIN is used as loading control. (**D**) The quantification of relative CRIM protein level against α-TUBULIN protein from Western blot images using Image J software (n = 3). Each sample was pooled from five to eight mice. *** $P < 0.005$. (**E**) Western blot performed on the protein samples from the WT and *Yap1*$^{+/-}$ lens epithelia using indicated antibodies. (**F**) Relative FAK phosphorylation level normalized to the FAK protein level, and ERK1/2 phosphorylation signal relative to ERK1/2 total protein signal, were quantitated from Western blot images using Image J software (n = 3). Each sample was pooled from five to eight mice. * $P < 0.05$, *** $P < 0.005$. All values are expressed as the mean ± SD.

(Fig. 8F). Rescue of *Yap1*$^{+/-}$ LEC proliferation by ectopic expression of CRIM1 suggests that CRIM1 is a major downstream target of YAP1 in promotion of LEC proliferation.

Discussion

Yap1 encodes an evolutionarily conserved transcriptional coactivator, a downstream effector of the Hippo signaling pathway that controls tissue size and cell growth. It has been suggested that the gene plays a role in lens development.[30–33] Here, we report that heterozygous

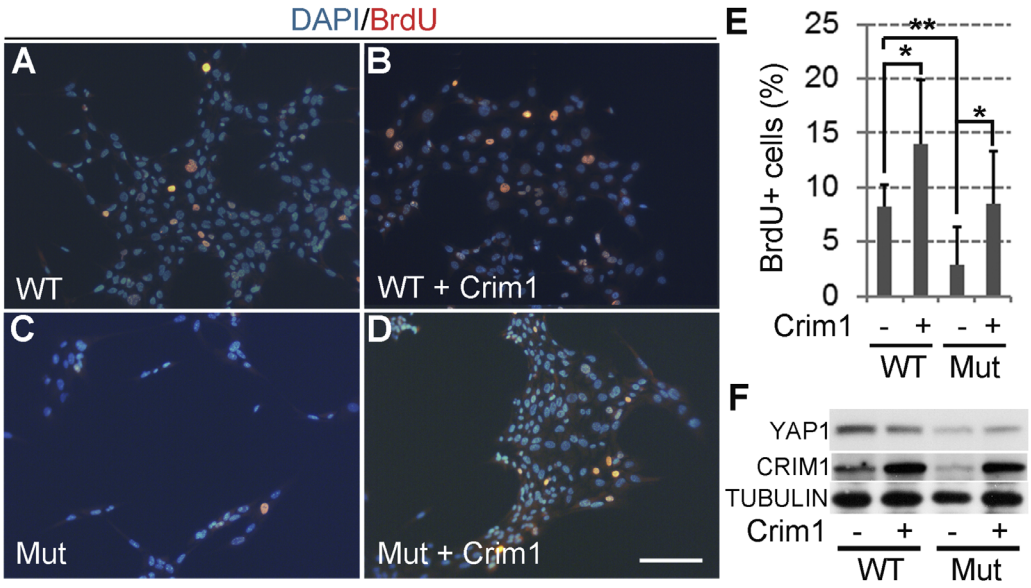

Figure 8. Rescue of the proliferation phenotype by overexpression of Crim1 in the primary *Yap1*$^{+/-}$ LECs. (**A–D**) The representative images of WT (**A**, **B**) and *Yap1*$^{+/-}$ (**C**, **D**) LECs transduced by lentiviral control vector (**A**, **C**) or lentiviral Crim1-expressing vector (**B**, **D**). Two days after transduction, the LEC culture medium was replaced with warm and fresh prepared medium containing 10 µM BrdU for two hours. After brief rinsing with phosphate-buffered saline solution, the LEC was fixed and processed for anti-BrdU immunostaining (*red*), and nuclei were counterstained with DAPI (*blue*). *Scale bar:* 100 µm. (**E**) Quantification of BrdU-positive cells in the indicated groups. Data are expressed as mean ± SD, n = 3 repeats. * $P \leq 0.05$, ** $P \leq 0.01$. (**F**) Western blot analysis of the YAP1, CRIM1, and α-TUBULIN protein levels in the indicated samples as (**A–D**).

inactivation of *Yap1* in mice induced cataracts caused by defects in LEC during adulthood. In the first month after birth, *Yap1*$^{+/-}$ mice showed a significant decrease in LEC cell density and focal breakage of cellular adhesion. Between two to three months of age, *Yap1*$^{+/-}$ mice showed more intensive damage to the integrity of LEC with a continuing decrease in cell density, which was followed by a widely observed cortical degeneration and opacification. YAP1 regulates the expression of cell-proliferative and anti-apoptotic genes. Conditional ablation of the *Yap1* gene reduced lens epithelial proliferation and increased apoptosis in the developing mouse lens in another study.[32] Interestingly, in the present study, we found that heterozygous inactivation of Yap1 gene in mice only affected LEC proliferation but not cell death, suggesting that YAP1 regulates LEC proliferation and survival via two different pathways and in a gene dose-dependent manner. A recent study also showed that *Yap1* conditional knockout mice developed cataracts with reduced LEC proliferation, however whether or not the LEC apoptosis had also been affected was not clear.[31] From a therapeutic perspective, inhibition of YAP1 activity could potentially be used as an anti-cancer therapy to limit both cancer growth and metastasis.[56] Our finding on the regulation of adult lens homeostasis by YAP1 expression highlights the importance of balancing Yap1 activity in vivo. Our results suggest comprehensive evaluations and better understanding of the potential side effects for systematical therapeutic blockage of YAP1 activity are warranted.

Mouse lenses with conditionally ablated *Yap1* showed that *Yap1*-deficient LECs precociously exited the cell cycle and fiber cells maintained relatively normal expression of the differentiation marker, β-crystallin.[32] Inhibition of YAP with Verteporfin in a lens epithelial explant model in vitro ablated cell elongation but preserved β-crystallin expression during lens fiber differentiation.[33] In our present study, *Yap1*$^{+/-}$ lenses showed disorganized alignment and packing of the fiber cells, while the β-crystallin expression was maintained. The underlying molecular mechanism leading to defective lens fiber morphogenesis in the *Yap1*$^{+/-}$ mice is currently unknown. It has been speculated that YAP1 might be involved in the junctional protein complex and actomyosin contraction, which could contribute to the phenotype by regulating cell migration and cell packing during lens fiber cell differentiation.[34,35,57]

Crim1 was previously identified as a direct transcriptional target of Yap1.[37–41] Both *Crim1* and *Yap1* mutant mice showed similar lens phenotypes in cell polarity, proliferation, and adhesion.[43] In the present study, we found that the mRNA and protein levels of Crim1 in the *Yap1*$^{+/-}$ LEC were lower compared with WT LEC. Additionally, the phosphorylation level of FAK and ERK was also significantly reduced in the *Yap1*$^{+/-}$ LEC, consistent with the critical role that Crim1 plays in interacting with β1 integrin and phosphorylation of FAK and ERK that functions as downstream mediators of integrin signaling.[43] More importantly, restoration of Crim1 rescued the proliferation phenotype of *Yap1*$^{+/-}$ LEC in culture. We conclude that YAP1 mediates LEC proliferation mainly through transcriptional regulation of *Crim1*. CRIM1 also forms complexes with β-catenin and cadherin, and stabilizes cell-cell junctions.[58] Disruption of cell adhesion in *Yap1*$^{+/-}$ LEC could be directly related to compromised cell adhesion due to reduced YAP1 and CRIM1 levels compared with the levels of WT LEC. Whether Crim1 mediates other phenotypes observed in the *Yap1*$^{+/-}$ lens remains to be determined. Investigations that are more detailed are necessary to establish the underlying molecular mechanisms that the YAP1 and CRIM1 play in LEC.

Acknowledgments

Supported by National Institutes of Health Grants EY027033 and EY030225, an unrestricted institutional grant from Research to Prevent Blindness, NY, GN151619B, and the Robert W. Rounsavall, Jr. Family Foundation, Inc.

Disclosure: **Q. Lu**, None; **Y. Zhang**, None; **R.B. Kasetti**, None; **S. Gaddipati**, None; **N.K. CVM**, None; **D. Borchman**, None; **Q. Li**, None

References

1. Kuwabara T. The maturation of the lens cell: a morphologic study. *Exp Eye Res*. 1975;20:427–443.
2. Zampighi GA, Eskandari S, Kreman M. Epithelial organization of the mammalian lens. *Exp Eye Re8s*. 2000;71:415–435.
3. Piatigorsky J. Lens differentiation in vertebrates. A review of cellular and molecular features. *Differentiation*. 1981;19:134–153.
4. Cvekl A, Ashery-Padan R. The cellular and molecular mechanisms of vertebrate lens development. *Development*. 2014;141:4432–4447.
5. Ogino H, Yasuda K. Sequential activation of transcription factors in lens induction. *Dev Growth Differ*. 2000;42:437–448.
6. Bassnett S, Sikic H. The lens growth process. *Prog Retin Eye Res*. 2017;60:181–200.
7. Hughes JR, Levchenko VA, Blanksby SJ, Mitchell TW, Williams A, Truscott RJ. No turnover in lens lipids for the entire human lifespan. *Elife*. 2015;4:e06003.
8. Liu P, Edassery SL, Ali L, Thomson BR, Savas JN, Jin J. Long-lived metabolic enzymes in the crystalline lens identified by pulse-labeling of mice and mass spectrometry. *Elife*. 2019;8:e50170.
9. Shi Y, De Maria A, Lubura S, Sikic H, Bassnett S. The penny pusher: a cellular model of lens growth. *Invest Ophthalmol Vis Sci*. 2014;56:799–809.
10. Audette DS, Scheiblin DA, Duncan MK. The molecular mechanisms underlying lens fiber elongation. *Exp Eye Res*. 2017;156:41–49.
11. Chow RL, Lang RA. Early eye development in vertebrates. *Annu Rev Cell Dev Biol*. 2001;17:255–296.
12. Cvekl A, Zhang X. Signaling and gene regulatory networks in mammalian lens development. *Trends Genet*. 2017;33:677–702.
13. Lovicu FJ, McAvoy JW. Growth factor regulation of lens development. *Dev Biol*. 2005;280:1–14.
14. Yu FX, Zhao B, Guan KL. Hippo pathway in organ size control, tissue homeostasis, and cancer. *Cell*. 2015;163:811–828.
15. Huang J, Wu S, Barrera J, Matthews K, Pan D. The Hippo signaling pathway coordinately regulates cell proliferation and apoptosis by inactivating Yorkie, the Drosophila Homolog of YAP. *Cell*. 2005;122:421–434.
16. Cai J, Zhang N, Zheng Y, de Wilde RF, Maitra A, Pan D. The Hippo signaling pathway restricts the oncogenic potential of an intestinal regeneration program. *Genes Dev*. 2010;24:2383–2388.
17. Camargo FD, Gokhale S, Johnnidis JB, et al. YAP1 increases organ size and expands undifferentiated progenitor cells. *Curr Biol*. 2007;17:2054–2060.
18. Dong J, Feldmann G, Huang J, et al. Elucidation of a universal size-control mechanism in Drosophila and mammals. *Cell*. 2007;130:1120–1133.
19. Schlegelmilch K, Mohseni M, Kirak O, et al. Yap1 acts downstream of alpha-catenin to control epidermal proliferation. *Cell*. 2011;144:782–795.
20. Zhang H, Pasolli HA, Fuchs E. Yes-associated protein (YAP) transcriptional coactivator functions in balancing growth and differentiation in skin. *Proc Natl Acad Sci USA*. 2011;108:2270–2275.
21. Zhao R, Fallon TR, Saladi SV, et al. Yap tunes airway epithelial size and architecture by regulating the identity, maintenance, and self-renewal of stem cells. *Dev Cell*. 2014;30:151–165.
22. Morin-Kensicki EM, Boone BN, Howell M, et al. Defects in yolk sac vasculogenesis, chorioallantoic fusion, and embryonic axis elongation in mice with targeted disruption of Yap65. *Mol Cell Biol*. 2006;26:77–87.
23. Azzolin L, Panciera T, Soligo S, et al. YAP/TAZ incorporation in the beta-catenin destruction complex orchestrates the Wnt response. *Cell*. 2014;158:157–170.
24. Fossdal R, Jonasson F, Kristjansdottir GT, et al. A novel TEAD1 mutation is the causative allele in Sveinsson's chorioretinal atrophy (helicoid peripapillary chorioretinal degeneration). *Hum Mol Genet*. 2004;13:975–981.
25. Steinhardt AA, Gayyed MF, Klein AP, et al. Expression of Yes-associated protein in common solid tumors. *Hum Pathol*. 2008;39:1582–1589.
26. Hamon A, Masson C, Bitard J, Gieser L, Roger JE, Perron M. Retinal degeneration triggers the activation of YAP/TEAD in reactive Muller cells. *Invest Ophthalmol Vis Sci*. 2017;58:1941–1953.
27. Kitagawa M. A Sveinsson's chorioretinal atrophy-associated missense mutation in mouse Tead1 affects its interaction with the co-factors YAP and TAZ. *Biochem Biophys Res Commun*. 2007;361:1022–1026.
28. Oatts JT, Hull S, Michaelides M, Arno G, Webster AR, Moore AT. Novel heterozygous mutation in YAP1 in a family with isolated ocular colobomas. *Ophthalmic Genet*. 2017;38:281–283.
29. Williamson KA, Rainger J, Floyd JA, et al. Heterozygous loss-of-function mutations in YAP1 cause both isolated and syndromic optic fissure closure defects. *Am J Hum Genet*. 2014;94:295–302.
30. Zhang N, Bai H, David KK, et al. The Merlin/NF2 tumor suppressor functions through the YAP oncoprotein to regulate tissue homeostasis in mammals. *Dev Cell*. 2010;19:27–38.
31. He Q, Gao Y, Wang T, Zhou L, Zhou W, Yuan Z. Deficiency of Yes-associated protein induces cataract in mice. *Aging Dis*. 2019;10:293–306.
32. Song JY, Park R, Kim JY, et al. Dual function of Yap in the regulation of lens progenitor cells and cellular polarity. *Dev Biol*. 2014;386:281–290.
33. Dawes LJ, Shelley EJ, McAvoy JW, Lovicu FJ. A role for Hippo/YAP-signaling in FGF-induced lens epithelial cell proliferation and fibre differentiation. *Exp Eye Res*. 2018;169:122–133.
34. Porazinski S, Wang H, Asaoka Y, et al. YAP is essential for tissue tension to ensure vertebrate 3D body shape. *Nature*. 2015;521:217–221.
35. Maddala R, Mongan M, Xia Y, Rao PV. Calponin-3 deficiency augments contractile activity, plasticity, fibrogenic response and Yap/Taz transcriptional activation in lens epithelial cells and explants. *Sci Rep*. 2020;10:1295.
36. Kumar B, Chandler HL, Plageman T, Reilly MA. Lens stretching modulates lens epithelial cell proliferation via YAP regulation. *Invest Ophthalmol Vis Sci*. 2019;60:3920–3929.
37. Pattschull G, Walz S, Grundl M, et al. The Myb-MuvB complex is required for YAP-dependent transcription of mitotic genes. *Cell Rep*. 2019;27:3533–3546.
38. Lee JY, Chang JK, Dominguez AA, et al. YAP-independent mechanotransduction drives breast cancer progression. *Nat Commun*. 2019;10:1848.

39. Zeng H, Zhang Y, Yi Q, Wu Y, Wan R, Tang L. CRIM1, a newfound cancer-related player, regulates the adhesion and migration of lung cancer cells. *Growth Factors*. 2015;33:384–392.
40. Wang Y, Xu X, Maglic D, et al. Comprehensive molecular characterization of the Hippo signaling pathway in cancer. *Cell Rep*. 2018;25:1304–1317.
41. Riz I, Hawley RG. Increased expression of the tight junction protein TJP1/ZO-1 is associated with upregulation of TAZ-TEAD activity and an adult tissue stem cell signature in carfilzomib-resistant multiple myeloma cells and high-risk multiple myeloma patients. *Oncoscience*. 2017;4:79–94.
42. Wilkinson L, Kolle G, Wen D, Piper M, Scott J, Little M. CRIM1 regulates the rate of processing and delivery of bone morphogenetic proteins to the cell surface. *J Biol Chem*. 2003;278:34181–34188.
43. Zhang Y, Fan J, Ho JW, et al. Crim1 regulates integrin signaling in murine lens development. *Development*. 2016;143:356–366.
44. Mason KV, Halliwell RE, McDougal BJ. Characterization of lichenoid-psoriasiform dermatosis of springer spaniels. *J Am Vet Med Assoc*. 1986;189:897–901.
45. Beleggia F, Li Y, Fan J, et al. CRIM1 haploinsufficiency causes defects in eye development in human and mouse. *Hum Mol Genet*. 2015;24:2267–2273.
46. Zelenka PS, Gao CY, Saravanamuthu SS. Preparation and culture of rat lens epithelial explants for studying terminal differentiation. *J Vis Exp*. 2009;31:e1519.
47. Bannik K, Rossler U, Faus-Kessler T, et al. Are mouse lens epithelial cells more sensitive to gamma-irradiation than lymphocytes? *Radiat Environ Biophys*. 2013;52:279–286.
48. Xin Y, Lu Q, Li Q. 14-3-3sigma controls corneal epithelial cell proliferation and differentiation through the Notch signaling pathway. *Biochem Biophys Res Commun*. 2010;392:593–598.
49. Livak KJ, Schmittgen TD. Analysis of relative gene expression data using real-time quantitative PCR and the 2(-Delta Delta C(T)) Method. *Methods*. 2001;25:402–408.
50. Sambandam SAT, Kasetti RB, Xue L, Dean DC, Lu Q, Li Q. 14-3-3sigma regulates keratinocyte proliferation and differentiation by modulating Yap1 cellular localization. *J Invest Dermatol*. 2015;135:1621–1628.
51. Rafferty NS, Rafferty KA, Jr. Cell population kinetics of the mouse lens epithelium. *J Cell Physiol*. 1981;107:309–315.
52. Enzo E, Santinon G, Pocaterra A, et al. Aerobic glycolysis tunes YAP/TAZ transcriptional activity. *EMBO J*. 2015;34:1349–1370.
53. Kim M, Kim T, Johnson RL, Lim DS. Transcriptional co-repressor function of the hippo pathway transducers YAP and TAZ. *Cell Rep*. 2015;11:270–282.
54. Noguchi S, Saito A, Mikami Y, et al. TAZ contributes to pulmonary fibrosis by activating profibrotic functions of lung fibroblasts. *Sci Rep*. 2017;7:42595.
55. Tam OH, Pennisi D, Wilkinson L, et al. Crim1 is required for maintenance of the ocular lens epithelium. *Exp Eye Res*. 2018;170:58–66.
56. Zanconato F, Cordenonsi M, Piccolo S. YAP/TAZ at the roots of cancer. *Cancer Cell*. 2016;29:783–803.
57. Neto F, Klaus-Bergmann A, Ong YT, et al. YAP and TAZ regulate adherens junction dynamics and endothelial cell distribution during vascular development. *Elife*. 2018;7:e31037.
58. Ponferrada VG, Fan J, Vallance JE, et al. CRIM1 complexes with ss-catenin and cadherins, stabilizes cell-cell junctions and is critical for neural morphogenesis. *PLoS One*. 2012;7:e32635.

Investigative Ophthalmology & Visual Science